Journal of Environmental Radioactivity 208-209 (2019) 106037

Contents lists available at ScienceDirect

Journal of Environmental Radioactivity

journal homepage: www.elsevier.com/locate/jenvrad

Design considerations for future radionuclide aerosol monitoring systems

Harry S. Miley[a], Jonathan L. Burnett[a], Ariane B. Chepko[b], Clive L. Devoy[b], Paul W. Eslinger[a,*], Joel B. Forrester[a], Judah I. Friese[a], Lance S. Lidey[a], Scott J. Morris[a], Brian T. Schrom[a], Sheldon Stokes[b], Michael E. Swanwick[b], John E. Smart[a], Glen A. Warren[a]

[a] Pacific Northwest National Laboratory, 902 Battelle Blvd, Richland, WA, 99354, USA
[b] Creare, 16 Great Hollow Road, Hanover, NH, 03775, USA

A B S T R A C T

Pacific Northwest National Laboratory (PNNL) staff developed the Radionuclide Aerosol Sampler Analyzer (RASA) for worldwide aerosol monitoring in the 1990s. Recently, researchers at PNNL and Creare, LLC, have investigated possibilities for how RASA could be improved, based on lessons learned from more than 15 years of continuous operation, including during the Fukushima Daiichi Nuclear Power Plant disaster. Key themes addressed in upgrade possibilities include having a modular approach to additional radionuclide measurements, optimizing the sampling/analyzing times to improve detection location capabilities, and reducing power consumption by using electrostatic collection versus classic filtration collection. These individual efforts have been made in a modular context that might constitute retrofits to the existing RASA, modular components that could improve a manual monitoring approach, or a completely new RASA. Substantial optimization of the detection and location capabilities of an aerosol network is possible and new missions could be addressed by including additional measurements.

1. Introduction

1.1. Historical basis

For decades, radioactive isotopes have been monitored in the atmosphere to protect populations from hazards associated with civilian nuclear processes and look for evidence of nuclear explosions (Maceira et al., 2017). The historical measurement strategy often collected a large-volume sample over several days, let the ubiquitous natural radon progeny in the sample decay for one to two weeks, and then measured the isotopes in the sample with a very sensitive detector, possibly using chemical separation to augment the selectivity of the radiometric system. Because atmospheric transport modeling was immature in the 1950s when atmospheric nuclear monitoring began, model-derived source strength estimates were deemphasized and isotopic ratio analysis was important. If a substantial fission product spectrum was present, ratios of isotopes could identify the time fission occurred, or the burnup of the reactor fuel involved in an accident. These determinations could be used to corroborate seismic signals of an explosion or news reports of a reactor issue to link the air parcel with the source, even without sophisticated transport models.

While many features of this process have improved, especially atmospheric transport calculations, the same ideas are used in environmental radioactivity networks today. An example is the informal European Network known as the Ring of Five (Ro5) (Masson et al., 2011), which is a network of completely manual aerosol collection and measurement capabilities. The Ro5 includes high-volume, high-sensitivity systems.

The creation of a global verification regime called the International Monitoring System (IMS) (CTBTO, 2019), for the Comprehensive Nuclear-Test-Ban Treaty (Comprehensive Nuclear-Test-Ban Treaty, 1996) drove the development of automated systems. The IMS requirements (National Research Council, 2012) (Table 2.9, page 57) and (Werzi, 2009) specified a three-day cycle for samples, with a 24-h sampling period, a 24-h waiting period for radon progeny decay, and a 24-h measurement period. Besides improving timeliness, the shorter sampling period led to smaller possible source regions calculated by atmospheric transport modeling (ATM). An inevitable consequence was that a shorter radon progeny decay period and measurement time led to poorer detection limits than the previous generation of manual systems and the Ro5 systems.

The Radionuclide Aerosol Sampler/Analyzer (RASA) (Miley et al., 1998) was developed in the 1990s to meet the IMS requirements. With 1000 m^3/h air flow, and the sample filter wrapped around a large radiation detector, the RASA achieves the required minimum detectable concentration (MDC) of 10 μBq/m^3 of ^{140}Ba in the atmosphere. Some

* Corresponding author. Pacific Northwest National Laboratory, MSIN K7-76, 902 Battelle Boulevard, Richland, WA, 99354, USA.
E-mail addresses: harry.miley@pnnl.gov (H.S. Miley), jonathan.burnett@pnnl.gov (J.L. Burnett), abc@creare.com (A.B. Chepko), cld@creare.com (C.L. Devoy), paul.w.eslinger@pnnl.gov (P.W. Eslinger), joel.forrester@pnnl.gov (J.B. Forrester), judah.friese@pnnl.gov (J.I. Friese), lance.lidey@pnnl.gov (L.S. Lidey), morris.scott@pnnl.gov (S.J. Morris), brian.schrom@pnnl.gov (B.T. Schrom), sxs@creare.com (S. Stokes), swanwick@creare.com (M.E. Swanwick), je.smart@pnnl.gov (J.E. Smart), glen.warren@pnnl.gov (G.A. Warren).

https://doi.org/10.1016/j.jenvrad.2019.106037
Received 3 May 2019; Received in revised form 24 August 2019; Accepted 26 August 2019

Ro5 manual systems achieve an MDC of 1 μBq/m^3 or less because they use extremely high-volume samples, optimized decay times, and high-efficiency sample-detector geometry. Nevertheless, the IMS systems can confidently measure releases more than 10 times smaller than the design criteria of releases from a 1-kt nuclear explosion in the atmosphere over the vast majority of the globe.

Since 1998, more than 250,000 aerosol samples have been measured in IMS operations. Factors that limit uptime of IMS aerosol systems have been studied, including component failures and power issues (Werzi, 2009). In addition, the IMS and the RASA in particular, were challenged by the aerosol emissions and power fluctuations from the Fukushima Daiichi Nuclear Power Plant disaster (Biegalski et al., 2012; Le Petit et al., 2014; Miley et al., 2013). Themes in operational lessons included determining the time of arrival of a large signal, needing early isotope information during a nuclear disaster, improving timeliness in reporting, and narrowing the possible source region of a source. A particular concern is reducing reliance on continuous power. A noted possibility is the use of electrostatic precipitation instead of air filtration, which can reduce power requirements and provide more responsive control of the sample acquisition process. Sampling stations at remote locations (e.g., island stations like Tristan de Cunha or Antarctic stations like Palmer Station) have little chance of sending an interesting sample back for timely laboratory analysis, so providing for automatic sample re-analysis after longer decay would be useful in some cases.

1.2. Adding capability to aerosol monitoring and implications for system requirements

The design arc for RASA and other IMS aerosol systems optimized them for a low-level underground nuclear explosion (UNE) release scenario and possibly the scenario of a very remote, very small atmospheric test. Fukushima signals are a reminder that a global network will have some systems that are relatively close to large signals, and should therefore measure key parameters of that phenomenology as well as the low-level release scenario. An alert from real-time detection of radioactivity in the airflow could allow controlling staff to adjust the operation of the system, and prepare for high-level samples. A three-day collect-decay-measure period is also of moderate value for reporting during a high-level event; a shorter collection time is highly desirable, if it can be done without degrading the system for the low-level scenario. Shorter collection times support an improved location estimation capability for atmospheric modeling, as well (Eslinger and Schrom, 2016).

Measuring short-lived isotopes at early times is also a valuable tool to help screen reactor emissions from nuclear explosions. Because the fission time in reactors is far longer than in explosions, the ratio of short and long half-life isotopes can show the source type. When the isotopes are shorter in half-life than the 10.6-h half-life of ^{212}Pb, a more sensitive approach is to measure them before decay occurs. As an example, consider looking at iodine ratios as a reactor/explosion screening indicator. It is also preferred to measure ratios within the same element to remove some of the uncertainty with how elements chemically react with the atmosphere. The 24-h decay period is not helpful for isotopes like ^{132}I, which has a half-life of 2.3 h. For example, the ratio of ^{132}I to ^{131}I with an 8-day half-life can give a strong discrimination between reactor debris and explosion debris. A 24-h decay period reduces the ^{132}I concentration on a sample by more than a factor of 1000. Considering the 24-h collection time, the ^{132}I could be suppressed by up to a factor of 10^6 before measurement begins. In Biegalski et al. (2012) the less sensitive ratio ^{133}I/^{131}I is used because the systems all had a 24-h decay in place. One order of magnitude separated the ratios for a reactor and an instantaneous fission. The measurement uncertainties in this case could have allowed a small admixture of explosion fission products with a larger reactor accident fission products without detection. Because the ^{133}I half-life (20.8 h) is about 10 times longer than ^{132}I, the authors posit that, had the same measurement been done without the 24-h decay, the ratio of ^{132}I/^{131}I, with the same measurement uncertainty, would have essentially eliminated the possibility of an explosive fission event.

It was noted above that the current IMS aerosol design focuses on a low-level UNE release scenario. IMS aerosol systems are sensitive to perhaps as few as 10 atoms of ^{131}I per cubic meter, versus the 3000 atoms of ^{133}Xe needed for IMS xenon systems. However, it may be no exaggeration to assume that xenon is 10^6 times more likely to be released than iodine, which leaves IMS aerosol systems 100 times less effective than xenon. To close this gap, and thus to contribute to xenon detection of some UNE leaks, the IMS aerosol systems could be made more sensitive to ^{131}I. Longer-lived isotopes like ^{131}I can be detected with about 10 times lower MDC after the air sample has had a week to decay. The authors calculate that an improvement of this magnitude would have allowed the detection of ^{131}I from the average U.S. underground nuclear test that leaked to the atmosphere (Aalseth et al., 2009; Miley et al., 2009). All of these functions can be supported by adding measurement modules to the RASA.

2. Trade-offs in the design of an aerosol monitoring system

2.1. Minimum detectable concentration

The key value that a monitoring system delivers is a stream of measurements that tightly limit the amount of emissions that could have been released without detection. For estimating this quantity, the lowest possible MDC is the key metric. While considering changes that would allow a system to meet IMS requirements, it is useful to consider a simple formula for the MDC, and introduce mitigating features to any change that would reduce the sensitivity of the system. The measurements are reported as a concentration with units of μBq/m^3; thus, the MDC is based on the minimum detectable activity.

In considering optimization of the system, we wish to determine the potential impact on the MDC of changes in key parameters of the system, such as sample collection time, decay time, sample measurement time, sample flow rate, and the measurement geometry. Given that sample times will be measured in hours, not minutes, we make the assumption that the background is associated with only the radon decay product ^{212}Pb with a halflife of 10.6 h and associated decay constant λ_B. Data from operational systems show that the background in an optimized energy window for ^{140}Ba, a key aerosol monitoring isotope, is > 100 counts in an island station with low ^{212}Pb, so an approximately 5% error is incurred if the constant 2.71 in Currie's working formula for paired observations (Currie, 1968) is omitted: $L_D \cong 4.65\sqrt{\mu_B}$.

Making a simplifying assumption that only ^{212}Pb Compton scatter events are responsible for the background in the energy region of interest, the width of which is some multiple of the Full Width at Half Max (FWHM) of the spectrometer. One can then write μ_B as a function of the ^{212}Pb concentration (Bq/m^3), detector resolution (keV), air volume V (m^3), collection time t_c (h), and a factor representing the detector efficiency, ε, and the solid angle the detector subtends from the source $\delta\Omega$.

$$\mu_B = \mathrm{C} \times [^{212}Pb\,] \times FWHM \times V \times t_C \times \varepsilon\delta\,\Omega \times e^{-\lambda_B t_d} \times \frac{(1 - e^{-\lambda_B t_C})}{\lambda_B}$$

Fig. 1 shows the RASA sample-detector geometry and some other possible geometries with better $\delta\Omega$. The constant of proportionality, C, in μ_B includes several terms, particularly those which convert the concentration of ^{212}Pb into counts per keV per unit time per cubic meter of air. The decay of ^{212}Pb is evaluated for a range of holding (decay) and counting times, t_d, and t_c, respectively. For an automated system with a single sampler and a single detector, the counting time equals the collection time, and so one symbol, t_c, can stand for both. A growth term that explicitly assumes a constant concentration in the air over the collection period was considered but not included because radon progeny concentrations have a wide natural diurnal variability. So this

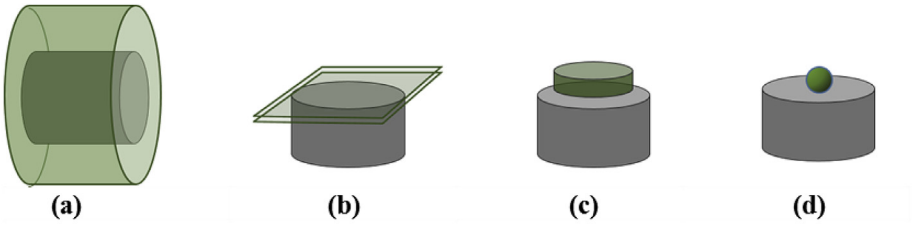

Fig. 1. Geometry comparison of (a) a RASA wrap-around geometry, (b) a 10-cm square, (c) a compressed puck, and (d) a point source. The RASA geometry factor, $d\Omega$, is about 5 times smaller than for a point source. The geometry factor for a 10-cm-square solid is 2 times smaller than for a point source.

MDC derivation considers only times from the end of the collection period to the end of the measurement period.

To construct an MDC for isotope A, the L_d minimum detectable counts are converted to a concentration using the gamma branching fraction, *Br*, the collected volume, *V*, measurement time, t_c, and the efficiency and solid angle, $\varepsilon\delta\Omega$. The following form is obtained:

$$MDC \cong \frac{4.65\sqrt{\mu_B}}{Br \times V \times t_c \times \varepsilon\delta\ \Omega \times e^{-\lambda_A t_d} \times \frac{(1-e^{-\lambda_A t_c})}{\lambda_A}}$$

The various decay terms represent the decay of isotope A, but this work specifically addresses ^{140}Ba with a halflife of 12.75 d. While the solid angle, $\delta\Omega$, will be the same for the 537.3 keV ^{140}Ba gamma decay and the ^{208}Tl gamma at 2614.5 keV from ^{212} Pb day, the efficiency ε will not. However, it understates the improvements shown in this work to use the same $\varepsilon\delta\Omega$ in both cases. Thus, expanding and collecting terms, we obtain:

$$MDC \cong C' \frac{\sqrt{e^{-\lambda_B t_d} \times \frac{(1-e^{-\lambda_B t_c})}{\lambda_B}}}{e^{-\lambda_A t_d} \times \frac{(1-e^{-\lambda_A t_c})}{\lambda_A}} \sqrt{\frac{[P_{212}b\ ] \times FWHM}{V \times t_c \times \varepsilon\delta\Omega}}$$

Possible ways to shorten the integration and measurement time from 24 h to 12, 8, or 6 h, while maintaining about the same MDC, include increasing *V* or $\varepsilon\delta\Omega$, or decreasing the measured background with more decay. With electrostatic precipitation (see Sec. 2.2), it may be possible to increase *V* and decrease power simultaneously. If the sample collection media is substantially thinner and more foldable than current RASA filters, an additional improvement in $\varepsilon\delta\Omega$ could be realized. If the notional design still used the maximum 72 h allowed by the IMS from start of sample collection to end of measurement, the time for decay of radon progeny could be substantially increased. Thus, an optimal design could potentially simultaneously shorten measurement time *t*, increase *V* or $\varepsilon\delta\Omega$, and decrease the measured background.

The relative effect of different design configurations on the MDC is shown in Table 1, where the current RASA performance is in row A. The MDC factors also use the assumption that the background counts are dominated by the presence of ^{212}Pb. This has been experimentally verified for continental stations, but there is less ^{212}Pb present in samples taken at island stations. Of course, improving $\varepsilon\delta\Omega$ by more than a factor of two, and tripling the air flow, results in a much better (lower) MDC in rows M, N, and O. Rows M and P show that with a folded sample geometry, as in Fig. 1b, a sampler could operate in a 12-h mode with the same MDC as the current 24-h mode. Higher airflow in addition to a better sample-detector geometry could allow 8- or 6-h operation. Doubled airflow and the better geometry make the results in row T almost equivalent to today's MDC, where tripling the airflow as in row U improves over today's MDC. Increasing the airflow of the existing system could be done by simply resizing the air pump at the expense of using significantly more power. Using more power lowers the chance of using a battery backup to operate during extended power failures such as during the Fukushima Daiichi Nuclear Power Plant disaster. We show in the next section that more sample volume and lower power can be simultaneously achieved by replacing filtration with electrostatic deposition.

Table 1
Possible measurement schemes and the impact on MDC for samples with ^{212}Pb contributions to the background concentrations. The air flow rate and the MDC have been scaled to 1 for the current RASA, and ε dΩ, or the efficiency of the sample-detector geometry, is scaled to the efficiency of a point source on the detector face. Current RASA performance is given in Row A.

Row	Geometry	Flow Rate	Sample & Count (h)	Decay Time (h)	MDC Factor	**MDC Factor with Added Detector**
A	0.2	1	24	24	1.00	NA[a]
B	0.2	2	24	24	0.71	NA
C	0.2	3	24	24	0.58	NA
D	0.2	1	12	48	1.58	NA
E	0.2	2	12	48	1.12	NA
F	0.2	3	12	48	0.91	NA
G	0.2	1	8	56	2.40	NA
H	0.2	2	8	56	1.70	NA
I	0.2	3	8	56	1.39	NA
J	0.2	1	6	60	3.37	NA
K	0.2	2	6	60	2.38	NA
L	0.2	3	6	60	1.94	NA
M	0.5	1	24	24	0.63	0.45
N	0.5	2	24	24	0.45	0.32
O	0.5	3	24	24	0.37	0.26
P	0.5	1	12	48	1.00	0.71
Q	0.5	2	12	48	0.71	0.50
R	0.5	3	12	48	0.58	0.41
S	0.5	1	8	56	1.52	1.07
T	0.5	2	8	56	1.07	0.76
U	0.5	3	8	56	0.88	0.62
V	0.5	1	6	60	2.13	1.51
W	0.5	2	6	60	1.51	1.07
X	0.5	3	6	60	1.23	0.87

[a] The current filter wrap-around geometry in the RASA does not support adding an additional detector.

2.2. Electrostatic precipitator sampling

Increasing the air flow rate while reducing power requires reducing the friction losses in the filtration material. An electrostatic precipitator (ESP) is a natural way to accomplish that. An ESP can accommodate significantly increased flow volumes compared to other filter media. Increased flow volume results in increased measurement sensitivity and provides design flexibility. The open flow channels in an ESP result in very low pressure drops, and therefore require much less blower power than the comparable blowers needed for conventional filters. While ESPs require high voltages to operate, the current is very low so that the supplied electrical power is low. This approach to radionuclide collection will significantly reduce system power, increase sample air volume, and thus improve instrument detection sensitivity.

Electrostatic precipitation offers an approach to aerosol collection that can provide greater operational flexibility. The collection efficiency can be dynamically adjusted by controlling independent parameters such as flow rate and the electric field strength within the precipitator to enhance or reduce particle collection in real time, adjust to changing radionuclide activity conditions, and operate in a low-power mode. Remotely reducing the collection efficiency after collecting a few full-intensity samples might be an attractive option in the future. This would have been useful during the Fukushima Daiichi Nuclear Power Plant disaster because some of the samples that could have been

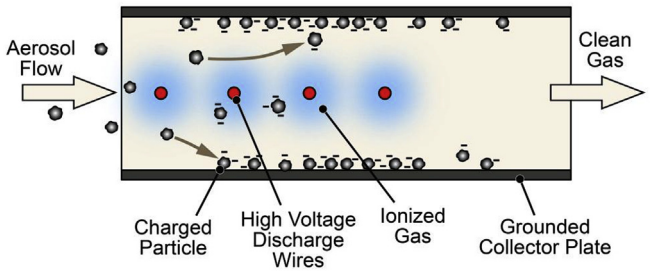

Fig. 2. Fundamental aspects of electrostatic precipitation operation.

obtained, between power outages, were too radioactive to ship or receive at a laboratory.

A standard wire-plate type ESP configuration is under investigation for application to radionuclide collection. In this approach, air is drawn through a precipitator volume that consists of a set of parallel rectangular flow channels. Along the center of each flow channel is a set of thin-wire discharge electrodes. A high voltage is applied to the discharge electrodes, which creates a strong electric field between the wires and the collection sheets. As air flows through the system, a corona of ionized gas molecules develops around each discharge electrode, which electrostatically charges the aerosol particles entrained in the flow, as shown in Fig. 2. Once charged, the particles are drawn by the electric field toward the collection sheets where they remain through a combination of electrostatic and van der Waals forces. The electrical force is countered by drag and dispersive turbulent forces on the particle. A challenge is that the design must have a sufficiently long flow residence time for the particle to build charge and migrate to the collector. Particle resistivity affects ESP performance, too high of resistivity can reduce electric field strength and lead to a back-corona discharge if the dust layer builds up too much; too low of resistivity results in easier re-entrainment of particles back into the flow. Typical atmospheric aerosol resistivity falls into the moderate-to-high range, although this varies with composition, temperature, and relative humidity.

A wide range of voltages, flow rates, ESP dimensions, and wire configurations have been tested to determine the impact on collection efficiency. Particle density and spectrometry measured before and after the collection chamber is a simple way to evaluate collection efficiency as a function of particle size, flow rate, and applied voltage. A parametric study of efficiency vs. flow rate, power level and various voltages was performed. The before and after particle density measurements determines that particles were removed but does not prove the particles were attached to the desired surface. However, in this case, the collection surface was essentially all of the available surface, so the authors feel confident that the differences are very small. In the future, this can be checked using airborne radioactivity.

The original idea of the RASA was to expose a number of small filter strips to air flow simultaneously, then physically concentrate these strips for measurement. The total filter size was large during collection, to minimize air velocity and drag, but then compact during gamma spectroscopy to maximize the gamma-ray detection efficiency. In the interior view of the radionuclide collector in Fig. 3, air flow would be from left to right, and during sample change, the aluminized collection medium would move downwards. Several of these ESP radionuclide collectors would be arranged in such a way that ducting would bring air to all of them, and wide strips of collection media would move from rolls, through the collectors, then to folding, and then to radiation sensors, as shown in Fig. 4.

Fig. 3. ESP radionuclide collector under development for this work. ESP can achieve very high collection efficiencies (> 99.5%) across a wide range (30 nm to > 100 μm) of particle sizes.

Because the likelihood of collecting a particle in a flow-through precipitator depends on the residence time of the particle in the ESP cell, and increasing the flow rate decreases the residence time, if one holds all other operating parameters constant, the ESP loses particle collection efficiency at high flow speeds. Even at a lower collection efficiency, because the sample volume can be much larger, the total amount of particulate collected can be much larger. The results provided in Fig. 5 are scaled such that one arbitrary unit of particles would be expected to be collected at the IMS minimum specification of 500 m^3/h and 80 percent particle collection efficiency. At double the flow rate, the same system might only have 60 to 70 percent flow-through particle collection efficiency, but the resulting amount of particulates could be 1.5 times larger. The operating voltage may be adjusted to recover some of the lost collection efficiency of high flow (as seen in Fig. 6), improving the amount of collected particulates to 2 or 3 times the minimum specification. This comes at the cost of increased power consumption, so a design needs to consider competing needs.

As an example, select a sampling power level of 1100 W, similar to the power used by the current RASA design. The curves in Fig. 6 indicate that with an applied voltage of 5 kV for ESP, a particle collection efficiency of 0.7 would be achieved with flow rate of 3000 m^3/h. Plotting this efficiency and flow in Fig. 5 would result in collecting 5 times the number of particulates as the IMS requirements and 2.5 times the number of particulates collected by today's RASA at the same power consumption.

2.3. Implications of using ESP on samples

The systems being researched use aluminized Mylar™ (registered trademark of DuPont Teijin) for a particulate collection surface. Many strips of exposed Mylar are collected together to form a sample. Many folding options are possible because the sample medium is less than 1-mm thick, compared to an approximately 1-cm thick RASA filter bundle. A simple modification to the wraparound geometry used in the RASA to make the sample 5 cm wide versus 10 cm wide could improve the sample-detector efficiency by around 5 percent. With more complex mechanical folding or limitations on the surface area of the Mylar, a 10-cm folded package (see Fig. 1) is possible, which could ultimately lead to a shorter residence time for particles in the ESP cell.

Aside from trade-offs in power, size, and detector geometry, aluminized Mylar is a substantially different sample medium than used in the past. The implications on radiometric measurement and sample dissolution chemistry are prudent to consider. A 42.9-g simulated Mylar blank sample bundle was measured in the Shallow Underground Laboratory at Pacific Northwest National Laboratory (PNNL) (Aalseth et al., 2012) with a Canberra Broad Energy Germanium (BEGe) detector in a configuration quite similar to Fig. 1c. The BEGe detector is equipped with a cosmic veto system (Burnett and Davies, 2014) that reduced the detector background by 25 percent. The sample was compressed into a cylinder (55 mm in diameter by 22 mm in height) and measured for eight days. The resulting gamma spectra analysis indicated trace levels of naturally occurring radionuclides from the ^{238}U and ^{232}Th series. As shown in Table 2, the activity of these radionuclides ranged from 3.7×10^{-4} Bq/g to 1.2×10^{-2} Bq/g. Although the quantity of aluminum is slight, many sources of aluminum are known to contain traces of ^{238}U and ^{232}Th (Wogman, 1981). Interestingly, these values are an order of magnitude lower and higher, respectively, than a similar measurement of this type of material 33 years earlier (Brodzinski et al., 1985). A comparison was made with a 40.0 g

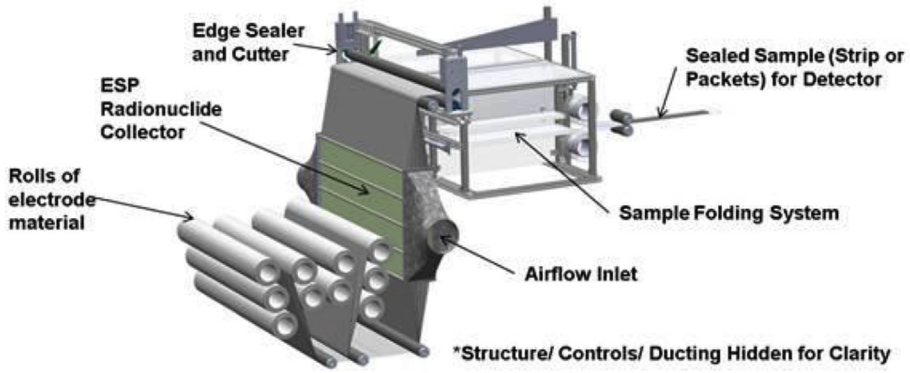

Fig. 4. Full-scale ESP concept, which adapts the multiplexed sampling concept of the RASA to electrostatic collection, using the ESP radionuclide collector seen in Fig. 3.

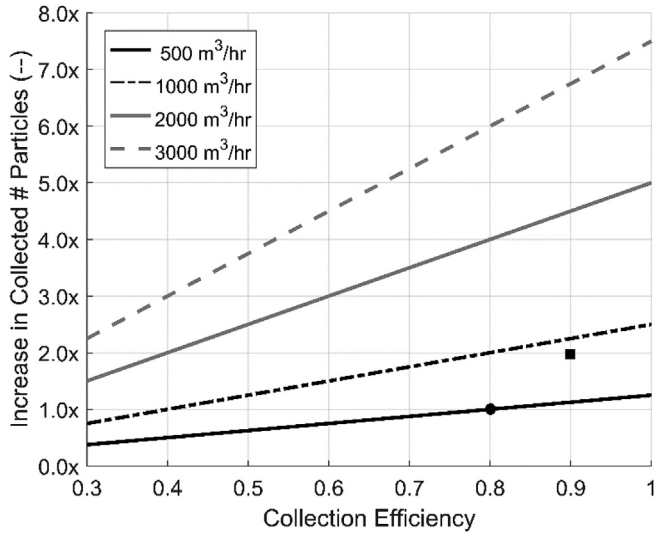

Fig. 5. Relative increase in modeled total number of collected particles over a baseline 12,000 m^3/d sample volume (500 m^3/h at 80 percent filter particle collection efficiency) for different flow rates and filter collection efficiency requirements. The black dot is the current IMS minimum specification and the black square is the existing RASA performance.

sample of blank, compressed RASA material, which was measured using a certified IMS gamma-spectrometer (Greenwood et al., 2017) in the Shallow Underground Laboratory for seven days. This sample showed only measurable ^{40}K at 2.6×10^{-4} Bq/g. All other radionuclides were below the MDC level, typically an order of magnitude lower than for the aluminized Mylar sample. This would indicate the aluminized Mylar contains an increased amount of intrinsic radioactivity, more than the current RASA collection media. The authors suspect that this increased level would not affect daily IMS samples, which have relatively high levels of radon-daughter concentrations, but would indeed affect laboratory measurements or a second, low-background measurement by a future RASA instrument. Additional investigation is needed to determine if this is a substantial effect or if it could be remedied by selecting an alternative aluminum source in the fabrication of the sample media. Alternatively, other conductive films can be investigated for use as sample media, including metallized plastic films using metals other than aluminum.

An IMS requirement originating from historic environmental monitoring practice indicates that IMS samples should be dissolvable. Historically, samples were dissolved and elements chemically separated to overcome the inability of first-generation radiation detectors to discern one isotope from another using gamma-energy analysis. This lack of selectivity has been addressed since the 1970s by the use of high-energy resolution detectors such as high-purity germanium (HPGe) (Greenwood et al., 2017) and more recently by the use of $\gamma-\gamma$ coincidence detection (Britton et al., 2015a, 2015b). While chemical separations may not be strictly necessary, it is still a desirable characteristic for enhanced laboratory analysis.

Chemical digestion experiments were done on aluminized Mylar using wet ash and dry ash approaches. At this time, it is difficult to render a full assessment of the suitability of aluminized Mylar from a chemical processing perspective. Based on the tests completed and historical process knowledge, this new material likely brings new

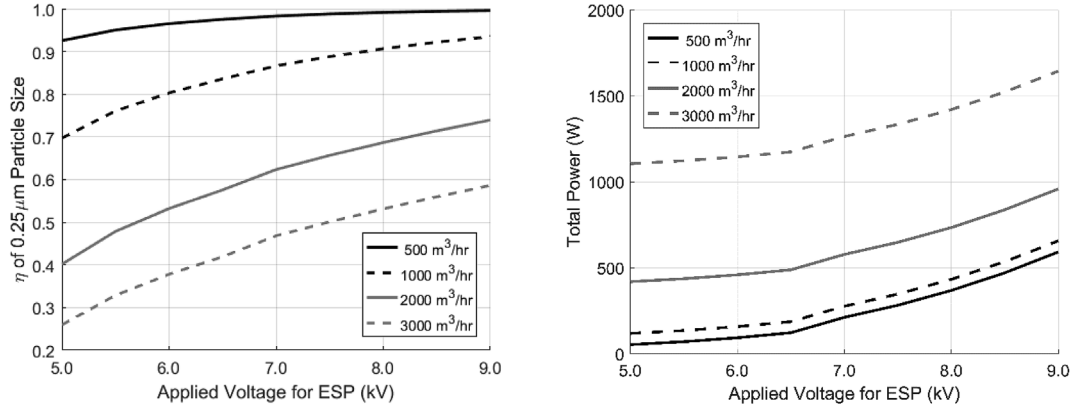

Fig. 6. Model predictions of collection efficiency versus ESP voltage for 0.25 μm diameter particles, which have the lowest efficiency rate. In other words, all other particles of interest have higher efficiency rates (left) and total power versus ESP voltage (right) for varying flow rates in an ESP design concept for radionuclide collection.

Table 2
Measured radionuclide concentrations and 2-σ uncertainties in an aluminized Mylar sample and standard RASA filter.

Nuclide	Energy (keV)	Aluminized Mylar		RASA Filter	
		Activity (Bq/g)	MDC (Bq/g)	Activity (Bq/g)	MDC (Bq/g)
^{40}K	1460.8	< MDC	3.5×10^{-3}	2.6×10^{-4} (53.1%)	4.5×10^{-4}
^{234m}Pa	1001.0	1.2×10^{-2} (12.1%)	6.7×10^{-3}	< MDC	2.5×10^{-3}
^{226}Ra	186.2		6.2×10^{-3}	< MDC	6.2×10^{-4}
^{214}Pb	351.9	1.4×10^{-3} (3.2%)	1.6×10^{-4}	< MDC	1.6×10^{-4}
^{214}Bi	1120.3	2.2×10^{-3} (7.1%)	6.0×10^{-4}	< MDC	2.0×10^{-4}
^{210}Pb	46.5	< MDC	2.9×10^{-3}	< MDC	4.1×10^{-3}
^{228}Th	84.4	6.0×10^{-3} (9.7%)	3.0×10^{-3}	< MDC	1.7×10^{-3}
^{228}Ac	911.2	< MDC	2.9×10^{-4}	< MDC	8.8×10^{-5}
^{224}Ra	241.0	6.4×10^{-3} (7.4%)	2.3×10^{-3}	< MDC	1.1×10^{-3}
^{212}Pb	238.6	< MDC	5.5×10^{-4}	< MDC	5.6×10^{-5}
^{212}Bi	727.3	< MDC	1.0×10^{-3}	< MDC	3.0×10^{-4}
^{208}Tl	2614.5	3.7×10^{-4} (10.9%)	1.2×10^{-4}	< MDC	2.6×10^{-5}
^{235}U	185.7	< MDC	3.9×10^{-4}	< MDC	3.9×10^{-5}

MDC = minimum detectable concentration.
RASA = Radionuclide Aerosol Sampler/Analyzer.

complications during chemical processing because of the large mass of aluminum in the material. The filter medium currently used in RASA units is known to dry ash down to an easily digestible solid after a lengthy dry-ashing procedure. The aluminized Mylar did not dry ash down to a similarly easily digestible solid. Several initial experiments were conducted to see if particulate material could be removed from the aluminized Mylar instead of total dissolution of the filter. Preliminary experiments indicate that it may be possible, but a more fundamental understanding of the interaction with the particulate matter with the aluminum is needed for a full assessment.

2.4. Nuclear detector options

In Fig. 7, four radiation detector positions are identified between the starting media roll and the sample archive media roll. Each of these represents an opportunity to tailor the radiation detection for the possible signals in a variety of signal scenarios (e.g., extremely elevated signals to extremely low-level signals) with multiple decay possibilities between each detector. Alternative detector choices are available to the HPGe detectors traditionally used. For example, a plastic scintillator could measure gross counts in the real-time position; a pair of NaI detectors, in coincidence configuration, could measure short-lived or high-intensity isotopes; one or more HPGe detectors could be employed in the classic IMS position; and a commercial ultra-low background detector with a cosmic veto system could perform the lab replacement measurement. In this notional design, the correct combination of detector choices could enhance mission capability, perhaps without major changes to the cost of a system.

A summary of comparisons among detectors for each aerosol monitoring role is provided in Table 3. Trade-off studies are required to determine how various mature and emerging radiation detectors could fulfill the role. As an example, one might consider that an upgraded real-time detector that measures isotopes, especially in a highly-concentrated sample, might eliminate the need for the early isotopes measurement. A highly upgraded detector in the Classic IMS position could greatly reduce the number of samples sent for laboratory analysis, or even eliminate the need for the laboratory replacement measurement. Operating a pair of detectors in the Classic IMS location would greatly reduce the remaining downtime in IMS operations, since if one failed, the nominal IMS MDC could still be maintained, with no loss of operational days. This comes at no added cost, since a duplicate detector is required to be present to minimize lost days.

If we consider only summing the single gamma ray detections from two identical detectors at the classic IMS location, we see in the rightmost column of Table 1 significantly enhanced MDC's are available for much shorter integration times. Added flow could reduce the integration time from 24 to 6 h. This exciting possibility requires the folded, 10 cm × 10 cm geometry sample of Fig. 1b. By employing coincidence, many other detection improvements could be realized.

A completely separate line of analysis is to consider dynamically changing operational modes in Table 1, say from row O to row V. Perhaps, a very high real-time signal could trigger a shift to very short integration times and eliminate the decay period, thus eliminating the need for the early isotope position. Such a change in programming could already be accomplished with today's automated IMS aerosol samplers with the addition of real-time detection capability to trigger the operations mode change.

3. Discussion and conclusions

The existing global IMS aerosol monitoring system was designed without the benefits of the last two decades of global monitoring experience and without today's relatively high-precision atmospheric models, data, and computational resources. These years of operations and data analysis have exposed the limitations of the network and shown opportunities for improving the aerosol instruments. During the

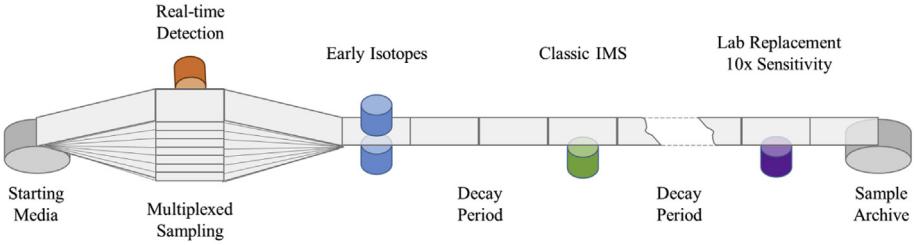

Fig. 7. Notional design for a next-generation aerosol monitoring system (not to scale). This concept shows four detector positions, including the original Classic IMS measurement position of the original RASA, but supports other signal scenarios by using additional radiation detectors.

Table 3
Obvious radiation detection choices and initial selections for new aerosol applications.

Fig. 7 Position *Application*	Obvious Detector *Main characteristic*	Improved Detector 1 *Main characteristic*	Improved Detector 2 *Main characteristic*
Real-time Detection *Time of arrival,*	Plastic scintillator *Basic high count rate*	Lanthanum halide *Some spectroscopy*	Dual small NaI crystals *High selectivity*
Early Isotopes *Short-lived species, timeliness*	Dual NaI 5x10x30 cm *High selectivity, efficiency*	Dual silicon or lanthanum halide *Higher selectivity, less efficiency*	Dual HPGe *Ultra-selectivity for complex samples*
Classic IMS *medium to low-level mission*	Single HPGe *IMS specifications*	Single HPGe w/cosmic veto *Better low-level sensitivity*	Dual HPGe *Ultra selectivity in complex spectra*
Lab Replacement *MC*	ULB HPGe w/cosmic veto. *Lab replacement*	Dual ULB HPGe w/cosmic veto. *Better than IMS labs*	

HPGe = high-purity germanium, IMS = International Monitoring System, MC = measurement confirmation, ULB = ultra low background.

past two decades, several announced nuclear tests, several announced accidental nuclear releases, and a major nuclear catastrophe occurred. These events have prompted deeper questions about instrument needs and how recent technology improvements can be used to answer them.

The source location capability of aerosol monitoring depends on atmospheric transport calculations, which in turn depend on a relatively accurate time component of the measurements (e.g., the arrival time and duration of a radioactive plume).

Question: Can *arrival time be measured?*

Answer: Arrival time of gross radioactivity can be easily measured, even as an add-on to existing aerosol monitoring systems.

Question: *Can sensitivity (low MDC) be maintained while shortening sample integration time?*

Answer: Table 1 shows that existing systems could be modified to accommodate shorter integration times, but enhanced sample-detector geometry allows both more sensitivity and shorter integration times. This work shows electrostatic deposition could provide both.

The current network is designed for a medium- to low-level scenario. Adapting this network to provide rapid discrimination capability in the high-level radionuclide release scenario would provide new capability in nuclear explosion monitoring, with a particular focus in confidently screening out civilian sources.

Question: *Can isotopes be identified and isotopic ratios measured with confidence at early times for large releases?*

Answer: Small, reasonably high-resolution radiation detectors operated individually, or in coincidence, should be able to discern the most basic characteristics of an intense plume of radioactivity. Fig. 7 shows this is possible in the Early Isotopes position and might even be possible in the Real-time Detection position in the air stream, although it would be a serious design challenge to arrange coincidence detectors around a collecting sample without adversely impeding airflow. In addition, electrostatic collection efficiency could be remotely reduced if sample activity exceeds bounds adopted to ensure safe handling and transport.

Improving the confidence, reliability, and ease of operation of stations would improve the overall monitoring value of the network. Marginal detections lead to unsatisfied users and many samples being sent to the laboratory for additional measurements, at high cost and long delay.

Question: *Could a field system be upgraded in a way to provide much of the advantages of a laboratory measurement of a sample?*

Answer: By employing a high-resolution coincidence measurement in place of the classic IMS measurement (high-resolution singles), some isotopic interferences can be removed so that the advantage of decay time before laboratory measurement or laboratory chemical separations is somewhat reduced. Perhaps as important, this measurement would provide results days to weeks earlier than current systems.

Question: *Can an automated field aerosol system use sufficiently less power such that it could be partially or completely battery-backed?*

Answer: Loss of power to mechanically cooled HPGe sensors specifically for this system component usually results in a lengthy warm–up/cool-down process. Simply providing an additional battery backup for this system could reduce the downtime of existing systems. However, rebuilding the system to use electrostatic deposition could reduce the power need for collections drastically, allowing complete system backup.

Question: *Could a field system be upgraded to eliminate the need for rapid transfer of a sample from the field to a laboratory (i.e., fill the laboratory need for remote sampling locations)?*

Answer: Commercial ultra-low background systems could be modified to accept automated sample transfers from an automated sampler/analyzer when the samples are appropriately aged, approximately one week after the classic IMS measurement, and provide much of the value of a laboratory re-measurement.

In this paper, these questions have been answered only to a notional level. It is clear that some of these concepts could be applied as upgrades to existing automated systems like the RASA, or possibly be applied in a modular way to manual systems. The optimal approach would be to simultaneously redesign all subsystems to achieve shorter sample integration time and more sensitivity, use less power, and support high- and low-level release scenarios. Changing all subsystems requires a complete redesign. The authors are aware that the MDC formula used in this work is not valid where ^{212}Pb is not the dominant half-life in the natural background spectrum of a sample, for example, sampling locations on islands where radon concentrations are comparatively low. The authors believe the potential has been firmly established for electrostatic deposition and radiation detection options, but more work is required to validate these notions and move to a conceptual design.

Acknowledgements

The authors are indebted to R. Britton and A. J. Davies for valuable insights and experience from testing the use of standby HPGe detectors in coincidence mode for the Classic IMS position. This option would add little new cost and reduce the downtime due to detector failures, and with a triggered operation change to eliminate decay, would fulfil the function of the Early Isotopes detector position. The authors acknowledge the support of the National Nuclear Security Administration Office of Defense Nuclear Nonproliferation and International Security, U.S. Department of Energy, for funding this work. Any subjective views or opinions expressed in the paper do not necessarily represent the views of the U.S. Department of Energy or the United States Government.

References

Aalseth, C., Andreotti, E., Arnold, D., Cabeza, J.-A.S., Degering, D., Giuliani, A., de Orduña, R.G., Gurriaran, R., Hult, M., Keillor, M., Laubenstein, M., le Petit, G., Margineanu, R.M., Matthews, K.M., Miley, H., et al., 2009. Ultra-low background measurements of decayed aerosol filters. J. Radioanal. Nucl. Chem. 282 (3), 731–735. https://doi.org/10.1007/s10967-009-0307-0.

Aalseth, C.E., Bonicalzi, R.M., Cantaloub, M.G., Day, A.R., Erikson, L.E., Fast, J., Forrester, J.B., Fuller, E.S., Glasgow, B.D., Greenwood, L.R., Hoppe, E.W., Hossbach, T.W., Hyronimus, B.J., Keillor, M.E., Mace, E.K., et al., 2012. A shallow underground laboratory for low-background radiation measurements and materials development. Rev. Sci. Instrum. 83 (11), 113503. https://doi.org/10.1063/1.4761923.

Biegalski, S.R., Bowyer, T.W., Eslinger, P.W., Friese, J.A., Greenwood, L.R., Haas, D.A.,

Hayes, J.C., Hoffman, I., Keillor, M., Miley, H.S., Moring, M., 2012. Analysis of data from sensitive U.S. Monitoring stations for the Fukushima Daiichi nuclear reactor accident. J. Environ. Radioact. 114, 15–21. https://doi.org/10.1016/j.jenvrad.2011.11.007.

Britton, R., Davies, A.V., Burnett, J.L., Jackson, M.J., 2015a. A high-efficiency HPGe coincidence system for environmental analysis. J. Environ. Radioact. 146, 1–5. https://doi.org/10.1016/j.jenvrad.2015.03.033.

Britton, R., Jackson, M.J., Davies, A.V., 2015b. Quantifying radionuclide signatures from a γ–γ coincidence system. J. Environ. Radioact. 149, 158–163. https://doi.org/10.1016/j.jenvrad.2015.07.025.

Brodzinski, R.L., Brown, D.P., Evans, J.C., Hensley, W.K., Reeves, J.H., Wogman, N.A., Avignone, F.T., Miley, H.S., 1985. An ultralow background germanium gamma-ray spectrometer. Nucl. Instrum. Methods Phys. Res. Sect. A Accel. Spectrom. Detect. Assoc. Equip. 239 (2), 207–213. https://doi.org/10.1016/0168-9002(85)90717-X.

Burnett, J.L., Davies, A.V., 2014. Cosmic veto gamma-spectrometry for comprehensive nuclear-test-ban treaty samples. Nucl. Instrum. Methods Phys. Res. Sect. A Accel. Spectrom. Detect. Assoc. Equip. 747, 37–40. https://doi.org/10.1016/j.nima.2014.02.027.

Comprehensive Nuclear-Test-Ban Treaty, 1996. Text of the comprehensive nuclear-test-ban treaty. United Nations Office for disarmament affairs (UNODA), status of multilateral arms regulation and disarmament agreements, CTBT. http://www.ctbto.org/the-treaty/treaty-text/, Accessed date: 20 September 2012.

CTBTO, 2019. Verification regime. http://www.ctbto.org/verification-regime/, Accessed date: 27 February 2019.

Currie, L.A., 1968. Limits for qualitative detection and quantitative determination: application to radiochemistry. Anal. Chem. 40 (3), 586–593. https://doi.org/10.1021/ac60259a007.

Eslinger, P.W., Schrom, B.T., 2016. Multi-detection events, probability density functions, and reduced location area. J. Radioanal. Nucl. Chem. 307 (3), 1599–1605. https://doi.org/10.1007/s10967-015-4339-3.

Greenwood, L.R., Cantaloub, M.G., Burnett, J.L., Myers, A.W., Overman, C.T., Forrester, J.B., Glasgow, B.G., Miley, H.S., 2017. Low-background gamma-ray spectrometry for the international monitoring system. Appl. Radiat. Isot. 126, 240–242. https://doi.org/10.1016/j.apradiso.2016.12.034.

Le Petit, G., Douysset, G., Ducros, G., Gross, P., Achim, P., Monfort, M., Raymond, P., Pontillon, Y., Jutier, C., Blanchard, X., Taffary, T., Moulin, C., 2014. Analysis of radionuclide releases from the Fukushima dai-Ichi nuclear power plant accident Part I. Pure Appl. Geophys. 171 (3), 629–644. https://doi.org/10.1007/s00024-012-0581-6.

Maceira, M., Blom, P.S., MacCarthy, J.K., Marcillo, O.E., Euler, G.G., Begnaud, M.L., Ford, S.R., Pasyanos, M.E., Orris, G.J., Foxe, M.P., Arrowsmith, S.J., Merchant, B.J., Slinkard, M.E., 2017. Trends in Nuclear Explosion Monitoring Research & Development-A Physics Perspective, LA-UR-17-21274. Los Alamos National Laboratory, Los Alamos, NM (United States). https://doi.org/10.2172/1355758.

Masson, O., Baeza, A., Bieringer, J., Brudecki, K., Bucci, S., Cappai, M., Carvalho, F.P., Connan, O., Cosma, C., Dalheimer, A., Didier, D., Depuydt, G., De Geer, L.E., De Vismes, A., Gini, L., et al., 2011. Tracking of airborne radionuclides from the damaged Fukushima dai-Ichi nuclear reactors by European networks. Environ. Sci. Technol. 45 (18), 7670–7677. https://doi.org/10.1021/es2017158.

Miley, H., Bowyer, S., Hubbard, C., McKinnon, A., Perkins, R., Thompson, R., Warner, R., 1998. A description of the DOE radionuclide aerosol sampler/analyzer for the comprehensive test ban treaty. J. Radioanal. Nucl. Chem. 235 (1–2), 83–87. https://doi.org/10.1007/BF02385942.

Miley, H.S., Aalseth, C.E., Bowyer, T.W., Fast, J.E., Hayes, J.C., Hoppe, E.W., Hossbach, T.W., Keillor, M.E., Kephart, J.D., McIntyre, J.I., Seifert, A., 2009. Alternative treaty monitoring approaches using ultra-low background measurement technology. Appl. Radiat. Isot. 67 (5), 746–749. https://doi.org/10.1016/j.apradiso.2009.01.069.

Miley, H.S., Bowyer, T.W., Engelmann, M.D., Eslinger, P.W., Friese, J.A., Greenwood, L.R., Haas, D.A., Hayes, J.C., Keillor, M.E., Kiddy, R.A., Kirkham, R.R., Landen, J.W., Lepel, E.A., Lidey, L.S., Litke, K.E., et al., 2013. Measurement of Fukushima aerosol debris in Sequim and Richland, WA and Ketchikan, AK. J. Radioanal. Nucl. Chem. 296 (2), 877–882. https://doi.org/10.1007/s10967-012-2231-y.

National Research Council, 2012. The Comprehensive Nuclear Test Ban Treaty: Technical Issues for the United States. The National Academies Press, Washington, DC. https://doi.org/10.17226/12849.

Werzi, R., 2009. The operational status of the IMS radionuclide particulate network. J. Radioanal. Nucl. Chem. 282 (3), 749. https://doi.org/10.1007/s10967-009-0270-9.

Wogman, N., 1981. Natural contamination in radionuclide detection systems. IEEE Trans. Nucl. Sci. 28 (1), 275–281. https://doi.org/10.1109/TNS.1981.4331179.